Multidimensional Media-Based Modulation

Ali Tugberk Dogukan[†], Zehra Yigit[*], and Ertugrul Basar[†]
[†]CoreLab, Department of Electrical and Electronics Engineering, Koç University, Sariyer, 34450, Istanbul, Turkey.
[*]Istanbul Technical University, Faculty of Electrical and Electronics Engineering, Maslak, 34469, Istanbul, Turkey
E-mail: adogukan18@ku.edu.tr, yigitz@itu.edu.tr, ebasar@ku.edu.tr

***Abstract*—Media-based modulation (MBM) is a new and promising transmission scheme that employs reconfigurable antennas to create different channel fade realizations and appears as an emerging index modulation (IM) application. In this paper, we present a novel multiple-input multiple-output (MIMO) transmission scheme called multidimensional media-based modulation (M-MBM) by redesigning the classical Alamouti's space-time block coding (STBC) scheme with MBM through the use of the additional dimension of channel states. The error performance of the proposed M-MBM scheme is theoretically analyzed for correlated and uncorrelated channel states and a union bound is obtained for the average bit error probability (ABEP). Moreover, through computer simulations, the superior error performance of the M-MBM scheme over the emerging IM techniques is demonstrated.**

***Index Terms*—Index modulation (IM), media-based modulation (MBM), space-time block coding (STBC), spatial modulation (SM).**

I. Introduction

OVER the past decade, index modulation (IM) schemes that employ the building blocks of transmission systems, have emerged as promising transmission technologies with their low-cost and energy-efficient structures [1]. Spatial modulation (SM) [2], which exploits the indices of transmit antennas (TAs), is assumed to be the pioneer of IM transmission schemes. On the other hand, media-based modulation (MBM) [3], which is an emerging digital transmission scheme, creates different channel realizations by altering the status of its radio frequency (RF) mirrors to convey additional information bits, and appears as a promising IM technique. In recent years, there has been a growing interest in the MBM transmission scheme, and several MBM-based systems have been proposed. In order to achieve transmit diversity gain, a space-time block coding (STBC) based MBM system design, space-time channel modulation (STCM), is introduced in [4]. More recently, MBM system designs for full-duplex communications [5], multi-user systems [6], secrecy communications [7] and with imperfect channel state knowledge [8] have been developed.

In this paper, we introduce a novel MIMO transmission system called *multidimensional media-based modulation* (M-MBM), which extends the classical Alamouti's STBC by applying IM jointly for TAs and channel states to obtain further multiplexing gains. In the proposed M-MBM scheme, a pair of the available TAs equipped with RF mirrors is activated, and two M-ary phase shift keying modulation (PSK) symbols are independently transmitted through the selected channel states of these active TAs. Two M-MBM system designs are presented for the cases of non-overlapping and overlapping subsets of the activated TAs. For the non-overlapping M-MBM schemes, the classical Alamouti's STBC principle is directly applied. However, for the overlapping M-MBM schemes, since overlapping subsets of active TAs violate the transmit diversity gain of Alamouti's STBC, a novel and optimized STBC structure is developed. Since the inherent orthogonality of the classical Alamouti's STBC is preserved in the non-overlapping M-MBM schemes, a two-stage, low-complexity maximum likelihood (ML) detector is proposed. Moreover, theoretical error performance analysis of the M-MBM systems over correlated and uncorrelated channel statistics is performed and a closed-form upper bound expression for the average bit error probability (ABEP) is obtained. Furthermore, the bit error rate (BER) performance of the M-MBM scheme is compared with the existing single-input multiple-output MBM (SIMO-MBM) [3], classical Alamouti's STBC [9], STCM [4] and space-time block coded SM (STBC-SM) [10] systems for the same spectral efficiency.

The rest of the paper is organized as follows. In Section II, the system model of the M-MBM scheme is introduced. Our theoretical performance analysis is given in Section III. The error performance comparison of the proposed system with the reference systems is carried out in Section IV, and the paper is concluded with Section V.

II. System Model

The general system model of the proposed M-MBM scheme is shown in Fig. 1. In the M-MBM scheme, we use not only classical data symbols and TA indices as in the STBC-SM scheme but also channel state realizations to transmit information bits. The transmission matrix of Alamouti's STBC is given as

$$\mathbf{G} = \begin{bmatrix} x_1 & -x_2^* \\ x_2 & x_1^* \end{bmatrix} \tag{1}$$

where x_1 and x_2 are two M-PSK symbols, $(\cdot)^*$ denotes complex conjugate, and rows and columns are respectively considered for TAs and time intervals.

Let us consider a MIMO configuration with N_r receive antennas (RAs) and N_t TAs where each of the available N_t TAs is surrounded by m_{rf} RF mirrors that can generate $N = 2^{m_{rf}}$ channel state realizations. In the M-MBM scheme, the incoming information bits are split into three parts: the

This work was supported by the Scientific and Technological Research Council of Turkey (TUBITAK) under Grant 117E869. The work of E. Basar was supported by the Turkish Academy of Sciences GEBIP Programme.

978-1-7281-8903-1/20/$31.00 ©2020 IEEE

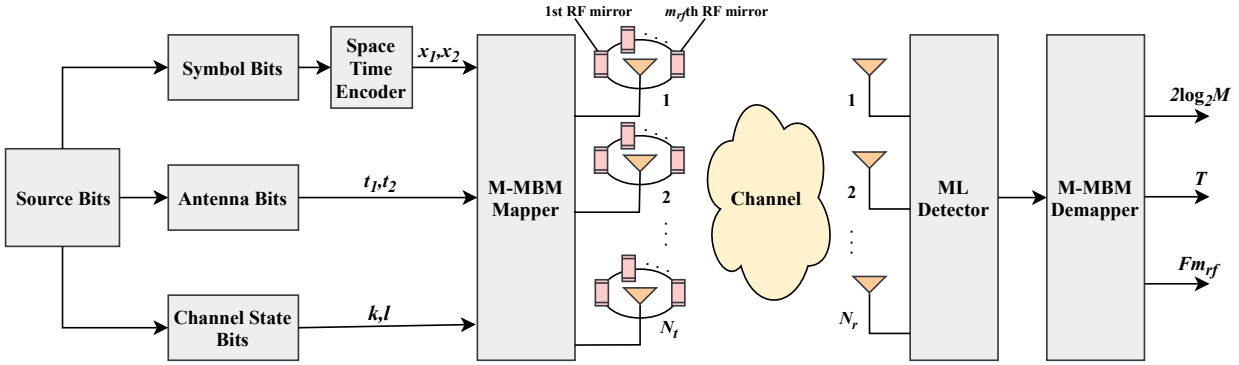

Fig. 1. System model of M-MBM scheme (F=1 for Scheme-I and F=2 for Scheme-II)

first bit sequence determines two M-PSK modulated symbols, x_1 and x_2, the second bit sequence determines the indices of active TAs t_1 and t_2, where $t_1, t_2 \in \{1, 2, \ldots, N_t\}$, and the last bit sequence determines the active channel states k and l, which correspond to active TAs with indices t_1 and t_2, respectively, to transmit x_1 and x_2 symbols in the first time slot. After applying Alamouti's STBC principle, the extended transmission matrix $\mathbf{S} \in \mathbb{C}^{NN_t \times 2}$ is constructed as

$$\mathbf{S} = \left[\begin{array}{c|c|c|c} \overbrace{0 \ \ldots \ 0}^{1} & \overbrace{0 \ \ldots \ \overset{\uparrow k}{x_1} \ \ldots \ 0}^{t_1} & \overbrace{0 \ \ldots \ \overset{\uparrow l}{x_2} \ \ldots \ 0}^{t_2} & \overbrace{0 \ \ldots \ 0}^{N_t} \\ 0 \ \ldots \ 0 & 0 \ \ldots \ \underset{\downarrow m}{-x_2^*} \ \ldots \ 0 & 0 \ \ldots \ \underset{\downarrow n}{x_1^*} \ \ldots \ 0 & 0 \ \ldots \ 0 \end{array}\right]^T \tag{2}$$

where m and n are considered to be the indices of the active channel states of the second time slot to transmit $-x_2^*$ and x_1^* symbols from the active TAs with indices t_1 and t_2, respectively, where $k, l, m, n \in \{1, \ldots, 2^{m_{rf}}\}$.

For the proposed M-MBM schemes, the Kronecker [11] and equicorrelation [3] models are considered to model the correlation between antennas and channel states, respectively. Therefore, a correlated extended channel matrix $\mathbf{C} \in \mathbb{C}^{N_r \times NN_t}$ is assumed to be modeled through an uncorrelated channel matrix $\tilde{\mathbf{C}} \in \mathbb{C}^{N_r \times NN_t}$ whose entries are independent and identically distributed (i.i.d.) complex Gaussian random variables with $\mathcal{C}(0,1)$ distribution, where $\mathcal{C}(\mu, \sigma^2)$ denotes the distribution of a complex Gaussian random variable with μ mean and σ^2 variance, as $\mathbf{C} = \mathbf{R}_r^{1/2} \tilde{\mathbf{C}} \mathbf{R}_t^{1/2}$. Here, $\mathbf{R}_r$ and $\mathbf{R}_t$ represent receive and transmit correlation matrices with dimensions of $N_r \times N_r$ and $NN_t \times NN_t$, respectively. The correlation coefficients among the channel states and antennas [3] are respectively given as ρ_a and ρ_b, where $0 < \rho_a, \rho_b < 1$.

Then, the matrix of received signals $\mathbf{Y} \in \mathbb{C}^{N_r \times 2}$ is given as

$$\mathbf{Y} = \mathbf{CS} + \mathbf{W} \tag{3}$$

where $\mathbf{W} \in \mathbb{C}^{N_r \times 2}$ is the matrix of additive white Gaussian noise (AWGN) samples whose entries are assumed to be independent complex Gaussian random variables that follow $\mathcal{CN}(0, N_0)$ distribution and $\mathbf{S}$ is the extended transmission matrix of M-MBM, which is defined in (2).

We propose two novel M-MBM schemes considering different channel state realizations of k, l and m, n to transmit x_1, x_2 and $-x_2^*$, x_1^*, respectively. In Scheme-I and Scheme-II, to provide diversity gain, channel state realizations are assumed:

Scheme I: $k = l = m = n$
Scheme II: $k = n$, $l = m$.

TABLE I
INDICES OF ACTIVE TAS (t_1 AND t_2) FOR THE NON-OVERLAPPING CASE AND $N_t = 8$

Bits	The index of the first active antenna (t_1)	The index of the second active antenna (t_2)
{0 0}	1	2
{0 1}	3	4
{1 0}	5	6
{1 1}	7	8

TABLE II
INDICES OF ACTIVE TAS (t_1 AND t_2) FOR THE OVERLAPPING CASE AND $N_t = 4$

Bits	CBs	CWs	t_1	t_2
{0 0}	$\mathcal{S}_1$	$\mathbf{S}_{11}$	1	2
{0 1}		$\mathbf{S}_{12}$	3	4
{1 0}	$\mathcal{S}_2$	$\mathbf{S}_{21}$	2	3
{1 1}		$\mathbf{S}_{22}$	4	1

Furthermore, we provide two different TA index selection procedures for both schemes considering the overlap of two active TA indices.

Spectral efficiencies of Scheme-I and Scheme-II are obtained, in terms of bits per channel use (bpcu), as follows:

Scheme I: $\eta = \log_2 M + 0.5T + 0.5m_{rf}$ [bpcu]
Scheme II: $\eta = \log_2 M + 0.5T + m_{rf}$ [bpcu]

where T is the total number of bits transmitted by TA indices.

For both non-overlapping M-MBM Scheme-I and Scheme-II, in order to keep the second order transmit diversity gain, first, we assume that the incoming $T = \log_2\left(\frac{N_t}{2}\right)$ bits of the overall 2η bits determine consecutive non-overlapping indices as given in Table I, i.e., $t_1 = 2i - 1$ and $t_2 = 2i$, for $i = 1, 2, \cdots, N_t/2$.

On the other hand, as given in Table II, we also consider the overlapping TA subsets that violate the inherent second order transmission diversity gain of Alamouti's STBC. For this case, an optimization is required to preserve the second

order transmit diversity gain, which will be discussed in the following subsection while the number of information bits conveyed through TA indices is defined as $T = \lfloor \log_2 \binom{N_t}{2} \rfloor$, where $\binom{\cdot}{\cdot}$ is binomial coefficient. It is worth noting that N_t does not need to be an integer power of two for this case.

A. Optimization of Overlapping M-MBM Schemes

In Table II, the overlapping TA case is considered for both M-MBM Schemes I and II for an example case of $N_t = 4$. For this case, the set of active TA indices, t_1 and t_2 and $\mathcal{S}_i$ for $i \in \{1, 2\}$ are the corresponding codebooks (CBs), which contain transmission matrices (codewords (CWs)) of $\mathbf{S}_{ij}$ for $j \in \{1, 2\}$. Unlike the non-overlapping cases, for the overlapping M-MBM schemes, $\lfloor \log_2 \binom{N_t}{2} \rfloor$ information bits specify one of the possible $2^{\lfloor \log_2 \binom{N_t}{2} \rfloor}$ TA pair combinations, while for the non-overlapping M-MBM schemes described above (Scheme-I and Scheme-II), $\log_2 \left(\frac{N_t}{2}\right)$ bits specify the indices of active TAs t_1 and t_2. As seen from Table II, while $\mathbf{S}_{11}$ and $\mathbf{S}_{12}$ do not have overlapping indices, they overlap with $\mathbf{S}_{21}$ and $\mathbf{S}_{22}$, and vice versa. In this study, in order to preserve the second order transmit diversity order for the overall system presented in Table II, for this specific example, we assume that for the incoming $\{1\,0\}$ and $\{1\,1\}$ bits, the corresponding constellation for $\mathcal{S}_2$ CWs are rotated with an angle of θ while the $\mathcal{S}_1$ CWs are directly transmitted. Otherwise, the columns of different CWs will interfere with each other and reduce transmit diversity order to one [10]. An extension to higher number of antennas is also possible and can be performed in a similar manner.

To determine the optimum rotation angle of θ, the minimum coding gain distance (CGD) [12] between the possible M-MBM transmission CWs, which is one of the main STBC design parameters, is considered. When the CW of $\mathbf{S}_{ij}$ is transmitted and $\hat{\mathbf{S}}_{ij}$ CW is incorrectly detected, the coding gain distance of the overlapping M-MBM schemes is evaluated as

$$\delta_{min}(\mathbf{S}_{ij}, \hat{\mathbf{S}}_{ij}) = \min_{\mathbf{S}_{ij}, \hat{\mathbf{S}}_{ij}} \det\left(\mathbf{S}_{ij} - \hat{\mathbf{S}}_{ij}\right)\left(\mathbf{S}_{ij} - \hat{\mathbf{S}}_{ij}\right)^H \quad (4)$$

where $(\cdot)^H$ denotes Hermitian transposition. Eventually, the optimum θ that maximizes δ_{min}, denoted by θ_{opt}, is obtained from (4) as

$$\theta_{opt} = \arg\max_{\theta} \delta_{min}(\mathbf{S}_{ij}, \hat{\mathbf{S}}_{ij}). \quad (5)$$

The non-overlapping and overlapping cases are considered for both M-MBM Schemes I and II. For both cases, the optimum rotation angle θ_{opt} is obtained for different signal constellations by doing a search between 0^o and 180^o angles as given in Fig. 2. In Fig. 2(a), for the M-MBM Scheme-I, the optimum θ_{opt} value that maximizes δ_{min} for BPSK, QPSK and 8-PSK modulated symbols are determined as 90^o, 35^o and 20^o, respectively. On the other hand, in Fig. 2(b), for the M-MBM Scheme-II, the optimum θ_{opt} corresponding to BPSK, QPSK and 8-PSK constellations are determined as 90^o, 35^o and 20^o, respectively. We consider PSK constellations for the proposed M-MBM schemes due to the fact that IM with PSK modulation outperforms IM with QAM [13].

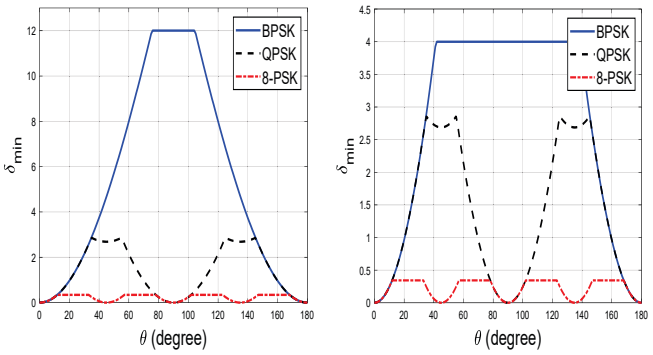

Fig. 2. Optimum θ_{opt} search for BPSK, QPSK and 8-PSK modulations for overlapping (a) M-MBM Scheme-I (b) M-MBM Scheme-II.

In the following, we describe the overlapping M-MBM Scheme-I transmission concept with a simple example.

Example (M-MBM Scheme-I): Suppose that the M-MBM Scheme-I with the system parameters of $N_t = 4$, $m_{rf} = 2$, and $M = 8$ achieves $\eta = 5$ bpcu, and a bit sequence of $\{1\,1\,1\,0\,1\,0\,1\,1\,1\,0\}$ with 2η length is transmitted. For this case, the first $2\log_2 M = \{1\,1\,1\,|\,0\,1\,0\}$ bit sequence specifies two 8-PSK symbols, $x_1 = -0.707 - 0.707j$ and $x_2 = -0.707 + 0.707j$, while the next $T = \{1\,1\}$ bits determine the indices of active TAs, which are $t_1 = 4$ and $t_2 = 1$ as given in Table II, and the last $m_{rf} = \{1\,0\}$ bits determine the index of the active channel state of the M-MBM Scheme-I, which corresponds to $k = l = m = n = 3$. As previously stated, for the overlapping M-MBM Schemes (Table II), when the CWs of $\mathbf{S}_{11}$ and $\mathbf{S}_{12}$ are considered, the transmission matrices are directly transmitted, while the other transmission matrices ($\mathbf{S}_{21}$ and $\mathbf{S}_{22}$) are rotated with an optimum angle of θ_{opt}. For the above example, since transmitted CW is $\mathbf{S}_{22}$ $(t_1 = 4, t_2 = 1)$ with 8-PSK, the overall transmission matrix is rotated with $\theta_{opt} = 20^\circ$ as obtained in Fig. 2(a). Therefore, the equivalent transmission matrix $\mathbf{S} \in \mathbb{C}^{16\times 2}$ with $x_1 = -0.707 - 0.707j$, $x_2 = -0.707 + 0.707j$ and $\theta_{opt} = 20^\circ$ is constructed as

$$\mathbf{S} = \left[\begin{array}{cccc|c|c|cccc} 0 & 0 & x_2 & 0 & \mathbf{0}_4 & \mathbf{0}_4 & 0 & 0 & x_1 & 0 \\ 0 & 0 & x_1^* & 0 & \mathbf{0}_4 & \mathbf{0}_4 & 0 & 0 & -x_2^* & 0 \end{array}\right]^T \times e^{\frac{j\pi 20^\circ}{180^\circ}} \quad (6)$$

where $\mathbf{0}_4$ represents an all-zero row vector that corresponds to inactive antenna elements.

B. M-MBM Detection

At the receiver side, the ML detection is considered and the transmitted signals $(\hat{x}_1, \hat{x}_2)$, their corresponding active TA indices $(\hat{t}_1, \hat{t}_2)$ and the active channel states $(\hat{k})$ and $(\hat{k}, \hat{l})$ are jointly detected for Scheme I and II, respectively, as

$$\left[\hat{x}_1, \hat{x}_2, \hat{t}_1, \hat{t}_2, \hat{k}\right] = \arg\min_{x_1, x_2, t_1, t_2, k} \|\mathbf{Y} - \mathbf{CS}\|_F^2 \quad (7)$$

$$\left[\hat{x}_1, \hat{x}_2, \hat{t}_1, \hat{t}_2, \hat{k}, \hat{l}\right] = \arg\min_{x_1, x_2, t_1, t_2, k, l} \|\mathbf{Y} - \mathbf{CS}\|_F^2 \quad (8)$$

where $\|\cdot\|_F$ is the Frobenius norm.

Additionally, to analyze the impact of the imperfect channel estimation, we assume that the receiver erroneously estimates the channel matrix $\mathbf{C}$ as $\hat{\mathbf{C}}$, which is in the form of $\hat{\mathbf{C}} = \mathbf{C} + \mathbf{E}$, where $\mathbf{C} = \tilde{\mathbf{C}}$ for $\rho_a = \rho_b = 0$, $\mathbf{E}$ is the error matrix, whose the entries are i.i.d. Gaussian random variables that follow $\mathcal{CN}(0, \sigma_E^2)$ distribution. Therefore, the entries of the overall estimated channel matrix $\hat{\mathbf{C}}$ are distributed with $\mathcal{CN}(0, 1 + \sigma_E^2)$.

Moreover, due to orthogonality of the columns of the Alamouti's STBC matrix (1), a further reduction in ML detection complexity [4], [10] is obtained by considering the following equivalent signal model

$$\mathbf{y}_{eq} = \mathbf{C}_{eq}\mathbf{s}_{eq} + \mathbf{w}_{eq} \tag{9}$$

where $\mathbf{y}_{eq} = [y_{1,1}\ \ y_{2,1}^*\ \ y_{1,2}\ \ y_{2,2}^* \cdots y_{1,N_r}\ \ y_{2,N_r}^*]^T \in \mathbb{C}^{2N_r \times 1}$ is the equivalent received signal vector, for $y_{a,b}$ being the received signal at time slot a and at RA b. $\mathbf{s}_{eq} = [x_1\ \ x_2]^T$ and $\mathbf{w}_{eq} \in \mathbb{C}^{2N_r \times 1}$ is the equivalent noise vector and $\mathbf{C}_{eq} = [\mathbf{c}_1\ \ \mathbf{c}_2] \in \mathbb{C}^{2N_r \times 2}$ equivalent channel matrix that is formed as in (10), where $h_{(t_1-1)N+k,n_r}$ and $h_{(t_1-1)N+m,n_r}$ represent the channel fading coefficient between the t_1th TA and n_rth RA for channel states k and m, respectively, while $h_{(t_2-1)N+l,n_r}$ and $h_{(t_2-1)N+n,n_r}$ represent the channel fading coefficient between the t_2th TA and n_rth RA for channel states l and n, respectively, for $n_r \in \{1, 2, \ldots, N_r\}$.

In the proposed M-MBM Scheme I, since the selection of the channel states is considered in a clever way, for the all possible realizations of the equivalent channel matrix $\mathbf{C}_{eq}$, $\mathbf{c}_1^H\mathbf{c}_2 = 0$ is satisfied. Therefore, it is possible to separately detect the transmitted symbols, x_1 and x_2, and the indices of the active TAs and their corresponding effective channel states. For M-MBM Scheme I, since $k = l = m = n$, the following minimum decision metrics are obtained through conditional ML detectors for all possible (k, t_1, t_2) realizations as follows

$$g_1^{(k,t_1,t_2)} = \min_{x_1} \|\mathbf{y}_{eq} - \mathbf{c}_1 x_1\|^2 \tag{11}$$

$$g_2^{(k,t_1,t_2)} = \min_{x_2} \|\mathbf{y}_{eq} - \mathbf{c}_2 x_2\|^2 \tag{12}$$

Hence, for all (k, t_1, t_2) realizations, the minimum ML decision metrics are obtained as $v^{(k,t_1,t_2)} = g_1^{(k,t_1,t_2)} + g_2^{(k,t_1,t_2)}$. Then a minimum metric selector determines the most likely $(\hat{k}, \hat{t}_1, \hat{t}_2)$ combination as follows

$$(\hat{k}, \hat{t}_1, \hat{t}_2) = \arg\min_{k,t_1,t_2} v^{(k,t_1,t_2)}. \tag{13}$$

After $(\hat{k}, \hat{t}_1, \hat{t}_2)$ combination is detected, the corresponding estimates of the modulated symbols x_1 and x_2 are obtained from (14) and (15).

For the M-MBM Scheme I, while the joint ML detector requires $2^T M^2 N$ metric calculations, this value is $2^{T+1}MN$ for the above two-stage optimum ML detector. On the other hand, for M-MBM Scheme II, the joint ML detector requires $2^T M^2 N^2$ metric calculations.

III. Theoretical Analysis of the M-MBM System

In this section, the error performance of the M-MBM scheme is analyzed and the ABEP of the system is obtained with the well-known union bounding technique [14]. Assuming that $\mathbf{S}_k$ is the matrix of transmitted signals and it is erroneously detected as $\hat{\mathbf{S}}_l$, we obtain an upper-bound on ABEP as

$$P_b \approx \frac{1}{2^{2\eta}} \sum_{k=1}^{2\eta} \sum_{l=1}^{2\eta} \frac{P(\mathbf{S}_k \to \hat{\mathbf{S}}_l) e(\mathbf{S}_k, \hat{\mathbf{S}}_l)}{2\eta}. \tag{14}$$

Here, 2η is the number of incoming data bits, $P(\mathbf{S}_k \to \hat{\mathbf{S}}_l)$ is the corresponding pairwise error probability (PEP) and $e(\mathbf{S}_k, \hat{\mathbf{S}}_l)$ is the number of bit errors. To obtain PEP, first, we derive a conditional PEP expression for the M-MBM schemes in terms of Q-function [14] as follows

$$P(\mathbf{S}_k \to \hat{\mathbf{S}}_l | \mathbf{C}) = Q\left(\sqrt{\Lambda / 2\sigma^2}\right) \tag{15}$$

where $\Lambda = ||\mathbf{C}(\mathbf{S}_k - \hat{\mathbf{S}}_l)||_F^2$. Assuming the difference matrix $\mathbf{\Omega} = (\mathbf{S}_k - \hat{\mathbf{S}}_l)(\mathbf{S}_k - \hat{\mathbf{S}}_l)^{\mathrm{H}}$, Λ can be written in the quadratic form as follows

$$\begin{aligned} \Lambda &= ||\mathbf{C}(\mathbf{S}_k - \hat{\mathbf{S}}_l)||_F^2 \\ &= \mathrm{Tr}\left(\mathbf{C}^{\mathrm{H}}(\mathbf{S}_k - \hat{\mathbf{S}}_l)(\mathbf{S}_k - \hat{\mathbf{S}}_l)^{\mathrm{H}}\mathbf{C}\right) \\ &= \mathrm{vec}(\tilde{\mathbf{C}}^{\mathrm{H}})^{\mathrm{H}}(\mathbf{R}_s{}^{1/2})^{\mathrm{H}}(\mathbf{I}_{N_r} \otimes \mathbf{\Omega})\mathbf{R}_s{}^{1/2}\mathrm{vec}(\tilde{\mathbf{C}}^{\mathrm{H}}) \end{aligned} \tag{16}$$

where $\mathbf{I}_{N_r}$ is an identity matrix with $N_r \times N_r$ dimensions, $\mathbf{R}_s = \mathbf{R_r} \otimes \mathbf{R}_t$, and $\otimes$, $\mathrm{vec}(\cdot)$ and $\mathrm{Tr}(\cdot)$ symbolize the Kronecker product, vectorization operator and trace of a matrix, respectively. Therefore, considering $Q(x) = \frac{1}{\pi}\int_0^{\pi/2} \exp(-x^2/2\sin^2\phi)\, d\phi$, the conditional PEP (15) is rewritten as

$$P(\mathbf{S}_k \to \hat{\mathbf{S}}_l | \mathbf{C}) = \frac{1}{\pi}\int_0^{\pi/2} \exp\left(-\psi \frac{\mathrm{vec}(\tilde{\mathbf{C}}^{\mathrm{H}})^{\mathrm{H}}\mathbf{\Delta}\mathrm{vec}(\tilde{\mathbf{C}}^{\mathrm{H}})}{4\sin^2\phi}\right) d\phi \tag{17}$$

where $\mathbf{\Delta} = (\mathbf{R}_s{}^{1/2})^{\mathrm{H}}(\mathbf{I}_{N_r} \otimes \mathbf{\Omega})\mathbf{R}_s{}^{1/2}$ and $\psi = 1/\sigma^2$. Then, the unconditional PEP expression is obtained by averaging (17) over $\mathbf{C}$ by considering the well-known moment generating function (MGF) approach

$$P(\mathbf{S}_k \to \hat{\mathbf{S}}_l) = \frac{1}{\pi}\int_0^{\pi/2} \mathcal{M}_{\mathbf{\Delta}}\left(-\frac{\psi}{4\sin^2\phi}\right) d\phi. \tag{18}$$

Since $\mathbf{\Delta}$ is in the quadratic form, the MGF in (18) can be calculated considering the following MGF expression for the quadratic form of $\mathbf{u}\mathbf{B}^{\mathrm{H}}\mathbf{u}$ [15]

$$\mathcal{M}(s) = \frac{\exp[s\bar{\mathbf{u}}^{\mathrm{H}}\mathbf{B}(\mathbf{I} - s\mathbf{Q_u}\mathbf{B})^{-1}\bar{\mathbf{u}}]}{\det(\mathbf{I} - s\mathbf{Q_u}\mathbf{B})} \tag{19}$$

where $\bar{\mathbf{u}}$ and $\mathbf{Q_u}$ is the mean vector and the covariance matrix of $\bar{\mathbf{u}}$, respectively. Let $\bar{\mathbf{u}} = \mathrm{vec}(\tilde{\mathbf{C}}^{\mathrm{H}})$ and $\mathbf{B} = \mathbf{\Delta}$. Since $\tilde{\mathbf{C}}$ is the Rayleigh fading channel matrix, $\bar{\mathbf{u}} = \mathrm{vec}(\tilde{\mathbf{C}}^{\mathrm{H}}) = \mathbf{0}$ and $\mathbf{Q_u} = \mathbf{I}_{NN_tN_r}$, respectively, the unconditional PEP of the system is evaluated from the following integral

$$P(\mathbf{S}_k \to \hat{\mathbf{S}}_l) = \frac{1}{\pi}\int_0^{\pi/2} \left[\det\left(\mathbf{I}_{NN_tN_r} + \frac{\psi}{4\sin^2\phi}\mathbf{\Delta}\right)\right]^{-1} d\phi. \tag{20}$$

After some simple manipulations, while considering uncorrelated channel statistics for $\mathbf{R}_s = \mathbf{I}_{NN_tN_r}$, and letting $\phi = \frac{\pi}{2}$,

$$\mathbf{C}_{eq} = \begin{bmatrix} h_{(t_1-1)N+k,1} & h^*_{(t_2-1)N+n,1} & \cdots & h_{(t_1-1)N+k,N_r} & h^*_{(t_2-1)N+n,N_r} \\ h_{(t_2-1)N+l,1} & -h^*_{(t_1-1)N+m,1} & \cdots & h_{(t_2-1)N+l,N_r} & -h^*_{(t_1-1)N+m,N_r} \end{bmatrix}^T \tag{10}$$

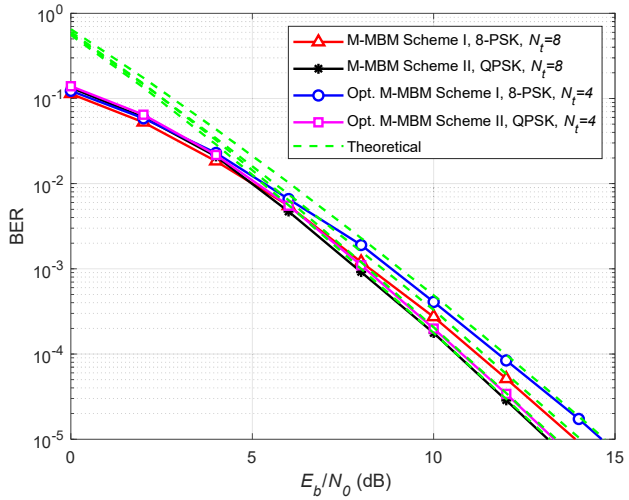

Fig. 3. Comparison of theoretical ABEP curves with Monte Carlo simulation results for M-MBM Schemes, $m_{rf} = 2$, $\eta = 5$ bpcu and $N_r = 2$.

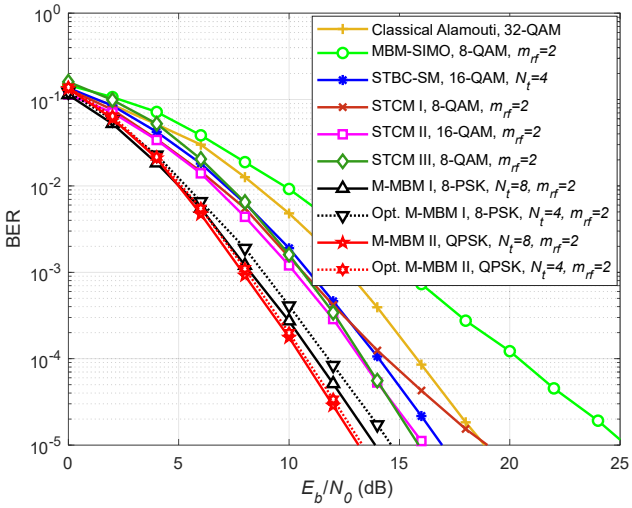

Fig. 4. Comparison of reference schemes with Monte Carlo simulation results for M-MBM Schemes, $\eta = 5$ bpcu and $N_r = 2$.

an upper bound for PEP is derived as follows:

$$P(\mathbf{S}_k \to \hat{\mathbf{S}}_l) \leq \frac{1}{2}\left[\left(1+\frac{\psi}{4}\lambda_1\right)\left(1+\frac{\psi}{4}\lambda_2\right)\right]^{-N_r} \tag{21}$$

where λ_1, λ_2 are the non-zero eigenvalues of difference matrix $\mathbf{\Omega}$.

IV. Simulation Results And Comparisons

In this section, the theoretical ABEP results of the proposed M-MBM scheme are given and supported through computer simulation results. All simulations are carried out with respect to average received energy per bit-to-noise ratio (E_b/N_0) and for $N_r = 2$. We consider Gray mapping for M-PSK modulated symbols and natural mapping for indices of TAs and channel states.

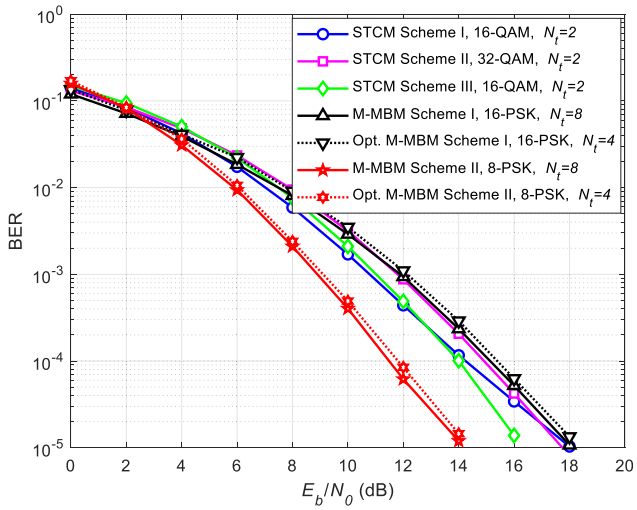

Fig. 5. Comparison of STCM schemes with Monte Carlo simulation results for M-MBM Schemes, $m_{rf} = 2$, $\eta = 6$ bpcu and $N_r = 2$.

In Fig. 3, the theoretical and computer simulation results for both overlapping and non-overlapping M-MBM schemes are given for $\eta = 5$ bpcu. It is observed from Fig. 3 that at high E_b/N_0 values, the theoretical and simulation results exactly coincide with each other. It is also observed that for both overlapping and non-overlapping cases, since the M-MBM Scheme-II requires a lower order M-PSK modulation at the same spectral efficiency, it achieves a considerably better error performance than the M-MBM Scheme-I. Moreover, for both Schemes I and II, since the overlapping cases are optimized for the maximum coding gain and transmit diversity, they exhibit nearly the same error performance with the non-overlapping schemes while using a less number of TAs.

In Fig. 4, the BER performance of the proposed M-MBM schemes is compared with the existing STBC-based transmission schemes for the spectral efficiency of $\eta = 5$ bpcu. It is clearly seen from Fig. 4 that the proposed M-MBM schemes exhibit a significantly better performance than the classical Alamouti's STBC [9], and respectively achieve 2 and 3 dBs E_b/N_0 gains over the existing STBC-based IM schemes: STCM [4] and STBC-SM [10].

To enrich our comparison, at $\eta = 6$ bpcu, the error performance of the M-MBM and outstanding STCM schemes is shown [4] in Fig. 5. Although M-MBM Scheme I is not able to yield superiority over STCM schemes due to the employment of a higher order modulation format, the M-MBM Scheme II provides 2 dB E_b/N_0 gain over STCM Scheme III and 4 dB E_b/N_0 gain over STCM Scheme II at a BER value of 10^{-5}.

In Fig. 6, at $\eta = 4$ bpcu, error performance of M-MBM schemes over correlated and uncorrelated channel conditions is shown. For the correlated channel states, in both the overlapping and non-overlapping M-MBM schemes, correlation

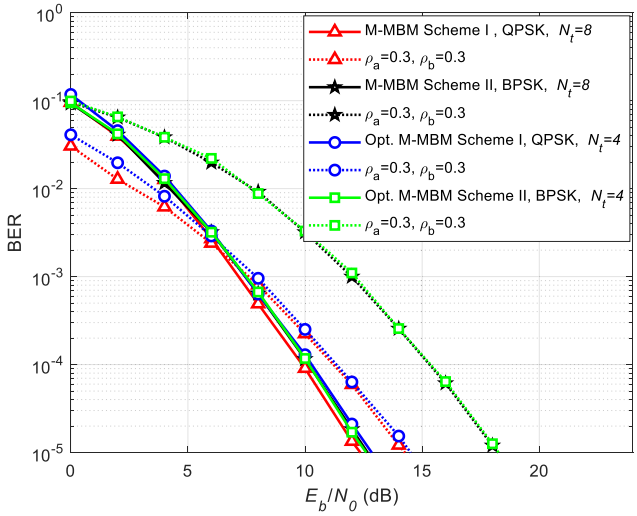

Fig. 6. Simulation results of the M-MBM schemes with correlated and uncorrelated channel states, $m_{rf} = 2$, $\eta = 4$ bpcu and $N_r = 2$.

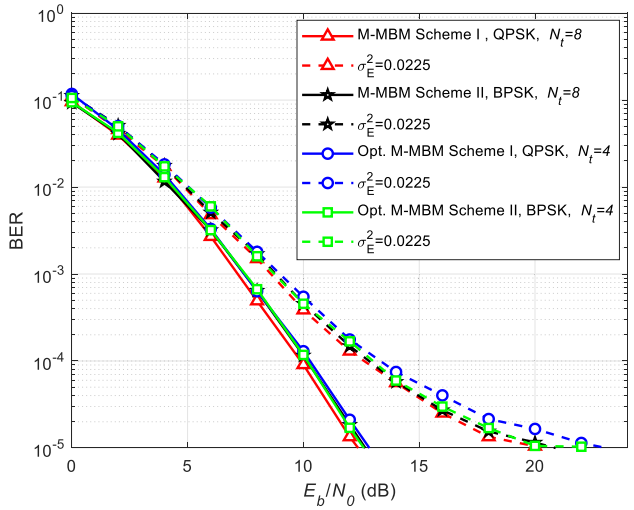

Fig. 7. BER performance of M-MBM schemes with perfect and imperfect channel estimation, $m_{rf} = 2$, $\eta = 4$ bpcu and $N_r = 2$ (no correlation among channel states and transmit antennas).

coefficients of $\rho_a = \rho_b = 0.3$ are considered. As seen from Fig. 6, at a BER value of 10^{-5}, the error performance of the correlated overlapping and non-overlapping M-MBM Scheme I, for $\rho_a = \rho_b = 0.3$, falls 2 dB behind uncorrelated cases. On the other hand, the error performance of the correlated overlapping and non-overlapping M-MBM Scheme II exhibits nearly 5 dB degradation compared to the uncorrelated cases. Therefore, we can deduce from the Fig. 6 that M-MBM Scheme I is more robust to the correlated channel conditions. MBM schemes is slightly better than the overlapping M-MBM schemes.

The error performance of the M-MBM schemes in the presence of channel estimation errors is investigated in Fig. 7. It is obviously seen from the Fig. 7 that when $\sigma_E^2 = 0.0225$ is assumed, the BER performance of the M-MBM scheme with imperfect channel estimation becomes significantly worse compared to the case of the perfect channel knowledge. On the other hand, in the presence of imperfect channel estimation, the error performance of the non-overlapping M-

V. Conclusion

In this paper, the M-MBM scheme has been presented as a novel STBC-based IM transmission concept for future wireless systems. To realize M-MBM, the concept of multidimensional IM has been considered by exploiting TAs and channel states in a joint manner. The error performance of the M-MBM scheme has been investigated in the presence of imperfect channel knowledge and correlated channel fading conditions. Moreover, the improved error performance of the M-MBM scheme over the existing STBC-based transmission systems has been demonstrated through Monte Carlo simulations. We conclude that the flexibility of the proposed system in reaching higher data rates while achieving satisfactory error performance makes it a potential candidate for future communication systems. On the other hand, generalization of the overlapping M-MBM scheme with multiple rotation angles is possible; however, left as a future work. Another interesting research direction would be the investigation of the proposed scheme with practical correlation and reconfigurable antenna models, which is also an open problem.

References

[1] E. Basar, "Index modulation techniques for 5G wireless networks," *IEEE Commun. Mag.*, vol. 54, no. 7, pp. 168–175, July 2016.
[2] R. Mesleh, H. Haas, S. Sinanovic, C. W. Ahn, and S. Yun, "Spatial modulation," *IEEE Trans. Veh. Technol.*, vol. 57, no. 4, pp. 22–28, July 2008.
[3] Y. Naresh and A. Chockalingam, "On media-based modulation using RF mirrors," *IEEE Trans. Veh. Technol.*, vol. 66, no. 6, pp. 4967–4983, June 2017.
[4] E. Basar and I. Altunbas, "Space-time channel modulation," *IEEE Trans. Veh. Technol.*, vol. 66, no. 8, pp. 7609–7614, Feb. 2017.
[5] Y. Naresh and A. Chockalingam, "Full-duplex media-based modulation," in *Proc. IEEE Globecom Workshops (GC Wkshps)*, Dec. 2017, pp. 1–6.
[6] M. Yüzgeçcioğlu and E. Jorswieck, "Performance of media-based modulation in multi-user networks," *Proc. the Int. Symp. Wireless Commun. Systems*, Aug. 2017.
[7] I. Yildirim, E. Basar, and G. Kurt, "Media-based modulation for secrecy communications," *IET Electron. Lett.*, vol. 54, pp. 789–791, June 2018.
[8] Y. Naresh and A. Chockalingam, "Performance analysis of media-based modulation with imperfect channel state information," *IEEE Trans. Veh. Technol.*, vol. 67, pp. 4192 – 4207, May 2018.
[9] S. M. Alamouti, "A simple transmit diversity technique for wireless communications," *IEEE J. Sel. Areas Commun.*, vol. 16, no. 8, pp. 1451–1458, Oct. 1998.
[10] E. Basar, U. Aygolu, E. Panayirci, and H. V. Poor, "Space-time block coded spatial modulation," *IEEE Trans. Commun.*, vol. 59, no. 3, pp. 823–832, Dec. 2011.
[11] A. Paulraj, R. Nabar, and D. Gore, *Introduction to space-time wireless communications*. Cambridge University Press, 2003.
[12] B. Vucetic and J. Yuan, *Space-time coding*. John Wiley & Sons, 2003.
[13] M. Di Renzo and H. Haas, "Bit error probability of SM-MIMO over generalized fading channels," *IEEE Trans. Veh. Technol.*, vol. 61, no. 3, pp. 1124–1144, Mar. 2012.
[14] M. K. Simon and M.-S. Alouini, *Digital communication over fading channels*. John Wiley & Sons, 2005.
[15] G. L. Turin, "The characteristic function of Hermitian quadratic forms in complex normal variables," *Biometrika*, vol. 47, no. 1/2, pp. 199–201, 1960.